Anisotropic Structure and Transport in Self-Assembled Layered Polymer−Clay Nanocomposites

Jodie L. Lutkenhaus,† Elsa A. Olivetti,‡ Eric A. Verploegen,‡ Bryan M. Cord,§ Donald R. Sadoway,‡ and Paula T. Hammond*,†

Departments of Chemical Engineering, Materials Science and Engineering, and Electrical Engineering, Massachusetts Institute of Technology, 77 Massachusetts Avenue, Cambridge, Massachusetts 02139

Received February 13, 2007. In Final Form: May 20, 2007

Using the layer-by-layer (LbL) assembly technique, we create a polymer−clay structure from a unique combination of LbL materials: poly(ethylene imine), Laponite clay, and poly(ethylene oxide). This trilayer LbL structure is assembled using a combination of hydrogen bonding and electrostatic interactions. The films were characterized using ellipsometry, profilometry, X-ray photon spectroscopy, atomic force microscopy, scanning electron microscopy, wide-angle X-ray diffraction, grazing-incidence small-angle X-ray scattering, and electrochemical impedance spectroscopy (EIS). We observe a layered, anisotropic structure, which resulted in in-plane ion transport 100 times faster than cross-plane at 0% relative humidity. This study represents a first application of EIS in determining anisotropic ion transport in LbL assemblies and its correlation to structural anisotropy.

Introduction

Synthetic clays are of interest for tuning bulk properties (rheological, mechanical, transport) at the nanoscale in the design of composite materials because of clay's unique materials properties (e.g., negative charge, silicate surface) and dimensions (e.g., nanoscale, platelet-shaped).[1] The high aspect ratio of the clay platelet is thought to yield superior transport barrier properties, particularly when oriented in layers.[2,3] Clay composites or clay-modified materials are often produced using mechanical pressure,[4] controlled drying from dilute solution,[5] or simple blending. Such systems may be of interest for diffusion blocking layers, mechanical modifiers, coatings, dielectrics, and so forth.

Montmorillonite and hectorite, both charged layer silicates (smectite clays), intercalated with poly(ethylene oxide) (PEO) and its derivatives have received much attention[4,6−20] as a single-ion conducting electrolyte owing to recent advances that demonstrate high conductivity and transference numbers near unity.[12−14] PEO complexes with and intercalates layered smectite clays through the competition of PEO and water binding to the clay platelet.[21,22] A well-studied polymer electrolyte, PEO associates with alkali cations through ion−dipole interactions, and cation mobility is influenced by local relaxations and segmental motion of the polymer backbone.[23,24] Early work with blended composites of PEO and montmorillonite demonstrated ionic conductivities (σ) of 10^{-9} to 10^{-7} S cm^{-1} at 425 K,[4,6,8] values much higher than montmorillonite alone. Adding a lithium salt such as lithium perchlorate can improve the room-temperature conductivity ($\sigma \approx 10^{-5}$ S cm^{-1}).[18] Addition of a plasticizer or small molecule such as ethylene carbonate can also improve performance ($\sigma \approx 10^{-4}$ S cm^{-1}),[12−14] but mechanical properties may suffer.

The use of ultrathin electrolytes allows reduction in overall electrolyte resistance, R, which scales with film thickness, L ($R = L/\text{area}\cdot\sigma$); thus, a film with a lower conductivity may provide a small resistance if made sufficiently thin. A simple and elegant way to construct ultrathin, mechanically cohesive polymer−clay nanocomposites is the layer-by-layer (LbL) technique.[25] Molecular species of opposite charge[26,27] (or hydrogen-bonding functionality)[28,29] are alternately adsorbed on a substrate from aqueous solution to form thin films of tunable thickness, structure, and properties.[26−29] Multilayers from positively charged polyelectrolytes and negatively charged clays have been studied as

* Corresponding author. E-mail: hammond@mit.edu.
† Department of Chemical Engineering.
‡ Department of Materials Science and Engineering.
§ Department of Electrical Engineering.

(1) Pinnavaia, T. J.; Beall, G. W. *Polymer-Clay Nanocomposites;* Wiley & Sons: Chichester, 2000.
(2) Struth, B.; Eckle, M.; Decher, G.; Oeser, R.; Simon, P.; Schubert, D. W.; Schmitt, J. *Eur. Phys. J. E* **2001**, *6* (5), 351−358.
(3) Kim, D. W.; Choi, H.-S.; Lee, C.; Blumstein, A.; Kang, Y. *Electrochim. Acta* **2004**, *50* (2−3), 659−662.
(4) Aranda, P.; Galvan, J. C.; Casal, B.; Ruiz-Hitsky, E. *Electrochim. Acta* **1992**, *37* (9), 1573−1577.
(5) Ghosh, P. K.; Bard, A. J. *J. Am. Chem. Soc.* **1983**, *105* (17), 5691−5693.
(6) Ruiz-Hitsky, E.; Aranda, P. *Adv. Mater.* **1990**, *2* (11), 545−547.
(7) Aranda, P.; Ruiz-Hitsky, E. *Chem. Mater.* **1992**, *4* (6), 1395−1403.
(8) Wu, J.; Lerner, M. M. *Chem. Mater.* **1993**, *5* (6), 835−838.
(9) Aranda, P.; Ruiz-Hitsky, E. *Acta Polym.* **1994**, *45* (2), 59−67.
(10) Doeff, M. M.; Reed, J. S. *Solid State Ionics* **1998**, *113−115*, 109−115.
(11) Chen, H.-W.; Chang, F.-C. *Polymer* **2001**, *42* (24), 9763−9769.
(12) Riley, M.; Fedkiw, P. S.; Khan, S. A. *J. Electrochem. Soc.* **2002**, *149* (6), A667−A674.
(13) Walls, H. J.; Riley, M. W.; Singhal, R. R.; Spontak, R. J.; Fedkiw, P. S.; Khan, S. A. *Adv. Funct. Mater.* **2003**, *13* (9), 710−717.
(14) Singhal, R. G.; Capracotta, M. D.; Martin, J. D.; Khan, S. A.; Fedkiw, P. S. *J. Power Sources* **2004**, *128* (2), 247−255.
(15) Kurian, M.; Galvin, M.; Trapa, P.; Sadoway, D. R.; Mayes, A. M. *Electrochim. Acta* **2005**, *50* (10), 2125−2134.
(16) Wong, S.; Vasudevan, S.; Vaia, R. A.; Giannelis, E. P.; Zax, D. B. *J. Am. Chem. Soc.* **1995**, *117* (28), 7568−7569.
(17) Vaia, R. A.; Vasudevan, S.; Krawiec, W.; Scanlon, L. G.; Giannelis, E. P. *Adv. Mater.* **1995**, *7* (2), 154−156.
(18) Chen, H.-W.; Chiu, C.-Y.; Chang, F.-C. *J. Polym. Sci., Part B: Polym. Phys.* **2002**, *40* (13), 1342−1353.
(19) Loyens, W.; Maurer, F. H. J.; Jannasch, P. *Polymer* **2005**, *46* (18), 7334−7335.
(20) Manoratne, C. H.; Rajapakse, R. M. G.; Dissanayake, M. A. K. L. *Int. J. Electrochem. Sci.* **2006**, *1* (1), 32−46.
(21) Parfitt, R. L.; Greenland, D. J. *Clay Miner.* **1970**, *8*, 305−315.
(22) Aray, Y.; Marquez, M.; Rodriguez, J.; Vega, D.; Simon-Manso, Y.; Coll, S.; Gonzalez, C.; Weita, D. A. *J. Phys. Chem. B* **2004**, *108* (7), 2418−2424.
(23) Tarascon, J.; Armand, M. *Nature* **2001**, *414*, 359−367.
(24) Gray, F. M. *Polymer Electrolytes;* Royal Society of Chemistry: Cambridge, 1997.
(25) Kleinfeld, E. R.; Ferguson, G. S. *Science* **1994**, *265* (5170), 370−373.
(26) Decher, G.; Hong, J. D.; Schmitt, J. *Thin Solid Films* **1992**, *210−211* (2), 831−835.
(27) Decher, G. *Science* **1997**, *277* (5330), 1232−1237.
(28) Stockton, W. B.; Rubner, M. F. *Macromolecules* **1997**, *30* (9), 2717−2725.
(29) Wang, L.; Wang, Z.; Zhang, X.; Shen, J.; Chi, L.; Fuchs, H. *Macromol. Rapid Commun.* **1997**, *18* (6), 509−514.

10.1021/la700432p CCC: $37.00
Published on Web 06/29/2007

surface modifiers, coatings, sensors, permeation barriers, and "artificial nacre".[3,25,30−43] In general, these layered organic−inorganic composites form a highly stratified two-dimensional structure,[25] which may be capable of blocking the diffusion of ions[2] or the permeation of gas.[3,35,42]

However, to explore applications in which the LbL polymer−clay composites may be part of an electrochemical device, we need to introduce and understand ionic conductivity. In this work, layered polymer−clay structures from LbL assembly are characterized and created using a unique combination of materials: PEO, linear poly(ethylene imine) (PEI), and neat or lithium-exchanged Laponite clay (designated as clay and Li-clay, respectively). Here, hydrogen bonding is used to introduce PEO into the multilayer film while using a polycation, PEI, to stabilize the composite. The resulting structure, studied using atomic force microscopy (AFM), scanning electron microscopy (SEM), wide-angle X-ray diffraction (WAXD), and grazing-incidence small-angle X-ray scattering (GI-SAXS), suggests lateral orientation over large areas (>4 cm^2). We demonstrate and characterize the degree of anisotropic ion transport using electrochemical impedance spectroscopy (EIS), and it was found that dry-state in-plane ionic conductivity (7.2×10^{-8} S cm^{-1} at 401 K) is 100 times higher than cross-plane conductivity (6.8×10^{-10} S cm^{-1} at 405 K), a result of the layered structure within the film. Thus, structural anisotropy within LbL polymer−clay composite films is correlated to anisotropic ion transport within the same film. To the best of our knowledge, this study represents the first application of EIS in determining anisotropic ion transport in LbL assemblies.

Experimental Section

Solution Preparation. Poly(ethylene oxide) of 4 000 000 molecular weight (MW) and linear poly(ethylene imine) of 25 000 MW were purchased from Polysciences. Polymer solutions of PEO and PEI were separately made using polymer and Milli-Q water. The concentration of polymer was 0.02 M based upon monomer unit. The pH of PEI solution was adjusted to 5.00 ± 0.01 using hydrochloric acid and a Beckman Coulter 390 pH meter.

Laponite RD, a synthetic hectorite, was purchased from EECS Cosmetics, and the manufacturer-reported diameter and thickness were ∼30 and ∼1 nm, respectively.[44] A dispersion of 0.5 wt % Laponite in Milli-Q water was made and stirred overnight. Laponite purchased from the manufacturer contained (exchangeable) sodium cations.[45]

Layer-by-Layer Film Assembly. Films were constructed using a modified programmable Carl Zeiss HMS slide stainer. Substrates used were silicon wafer and ITO-coated glass. Si wafers were cleaned using piranha solution of 70% sulfuric acid and 30% hydrogen peroxide. *CAUTION: Piranha solution is extremely corrosive.* ITO-coated glass substrates were cleaned by sequential sonication in dichloromethane, acetone, methanol, and Milli-Q water for 15 min each. Immediately before LbL assembly, the substrate was oxygen plasma-treated for 2 min. After plasma treatment, the substrate was first dipped in PEI solution for 10 min, rinsed with agitation in Milli-Q water for 2 min, followed by an additional 1-min rinse. Second, the substrate was exposed to the Laponite dispersion for 10 min and rinsed as before. Finally, the substrate was exposed to PEO solution for 10 min and rinsed as before. These three exposures comprise one trilayer of PEI/clay/PEO. The procedure can be repeated n times to give a film of n trilayers denoted by $(PEI/clay/PEO)_n$.

The film thickness was measured using either ellipsometry or profilometry depending on film thickness. Film thicknesses less than 150 nm were measured using a Gaertner ellipsometer. Film thicknesses greater than 150 nm were measured using a Tencor P-10 profilometer. The thickness was recorded three times on two different samples to give one data point.

X-ray Photon Spectroscopy. Surface characterization and elemental analysis were performed using a Kratos AXIS Ultra Imaging X-ray photoelectron spectrometer at 0.5 eV/step and 80 eV pass energy.

AFM. A Dimension 3100 AFM by DI Instruments with a Nanoscope 3A Controller in tapping mode was used to investigate surface morphology of LbL films assembled on silicon. NCH Pointprobe AFM cantilevers were purchased from Pacific Nanotechnologies.

SEM. Images were captured using a Carl Zeiss LEO field-emission SEM system operating between 1 and 5 keV. Two nanometers of Au−Pd was sputter-deposited on the samples before imaging to suppress charging. Cross section images were taken from samples cleaved using a diamond scribe.

WAXD. A Rigaku RU300 X-ray diffractometer (Cu Kα, $\lambda =$ 1.541 Å) was used for both powder diffraction and glancing angle WAXD. Powder diffraction of Laponite clay and thin film diffraction of the LbL assembly on silicon were conducted in ambient conditions (25 °C and 30% relative humidity). Scans were conducted from $2\theta = 3°$ to 50° at a rate of 0.01°/s.

GI-SAXS. Experiments were performed at the G1 beamline at the Cornell High Energy Synchrotron Source. The wavelength of the incident beam was 1.239 Å with a sample to detector distance of 1752 mm, and a 2-D area detector was used for data collection.[46]

Electrochemical Impedance Spectroscopy. Cross-plane impedance measurements were conducted using a cell described by DeLongchamp and Hammond.[47] Briefly, patterned ITO-coated glass (Donnelly and DCI) was used as the substrate for LbL assembly. Following LbL assembly atop the ITO-coated glass, gold electrodes (100-nm thick and 2-mm wide) were thermally evaporated using an Edwards Auto 306. Copper tape from 3 M was applied to the gold to form a contact pad. The active area was 6 mm^2.

In-plane conductivity measurements were performed on LbL films deposited on independently addressable microband electrodes (IAMEs) from Abtech Scientific. Each ITO band was 3-mm long with 5-μm width and spacing. The active area was given by 3 mm times the thickness of the LbL film.

Impedance measurements were performed using a Solartron 1260. The ac amplitude was 100 mV to improve the signal-to-noise ratio at high impedance. A linear sweep of the cross-plane and in-plane cells from −100 to 100 mV gave a linear current response, confirming that impedance measurements at this amplitude are appropriate.

(30) Ferguson, G. S.; Kleinfeld, E. R. *Adv. Mater.* **1995**, *7* (4), 414−416.
(31) Kleinfeld, E. R.; Ferguson, G. S. *Chem. Mater.* **1995**, *7* (12), 2327−2331.
(32) Kleinfeld, E. R.; Ferguson, G. S. *Chem. Mater.* **1996**, *8* (8), 1575−1578.
(33) Lvov, Y.; Ariga, K.; Ichinose, I.; Kunitake, T. *Langmuir* **1996**, *12* (12), 3038−3044.
(34) Kotov, N. A.; Haraszti, T.; Turi, L.; Zavala, G.; Geer, R. E.; Dekany, I.; Fendler, J. H. *J. Am. Chem. Soc.* **1997**, *119* (29), 6821−6832.
(35) Kotov, N. A.; Magonov, S.; Tropsha, E. *Chem. Mater.* **1998**, *10* (3), 886−895.
(36) MacNeill, B. A.; Simmons, G. W.; Ferguson, G. S. *Mater. Res. Bull.* **1999**, *34* (3), 455−461.
(37) van Duffel, B.; Schoonheydt, R. A.; Grim, C. P. M.; De Schryver, F. C. *Langmuir* **1999**, *15* (22), 7520−7529.
(38) Glinel, K.; Laschewsky, A.; Jonas, A. M. *Macromolecules* **2001**, *34* (15), 5267−5274.
(39) Glinel, K.; Laschewsky, A.; Jonas, A. M. *J. Phys. Chem. B* **2001**, *106* (43), 11246−11252.
(40) Tang, Z.; Kotov, N. A.; Magonov, S.; Ozturk, B. *Nat. Mater.* **2003**, *2* (6), 413−418.
(41) Vuillaume, P. Y.; Glinel, K.; Jonas, A. M.; Laschewsky, A. *Chem. Mater.* **2003**, *15* (19), 3625−3631.
(42) Ku, B.-C.; Froio, D.; Steeves, D.; Kim, D. W.; Ahn, H.; Ratto, J. A.; Blumstein, A.; Kumar, J.; Samuelson, L. A. *J. Macromol. Sci., Pure Appl. Chem.* **2004**, *41* (12), 1401−1410.
(43) Kim, D. W.; Blumstein, A.; Kumar, J.; Samuelson, L. A.; Kang, B.; Sung, C. *Chem. Mater.* **2002**, *14* (9), 3925−3929.
(44) Porion, P.; Faugere, A.-M.; Delville, A. *Eur. Phys. J. Special Topics* **2007**, *141*, 281−284.
(45) Southern Clay Products, Inc. *Laponite RD Product Bulletin*; Southern Clay Products: Gonzales, TX; http://www.scprod.com/product_bulletins/PB%20Laponite%20RD.pdf.
(46) Roe, R. J. *Methods of X-ray and Neutron Scattering in Polymer Science;* Oxford University Press: New York, 2000.
(47) DeLongchamp, D. M.; Hammond, P. T. *Chem. Mater.* **2003**, *15* (5), 1165−1173.

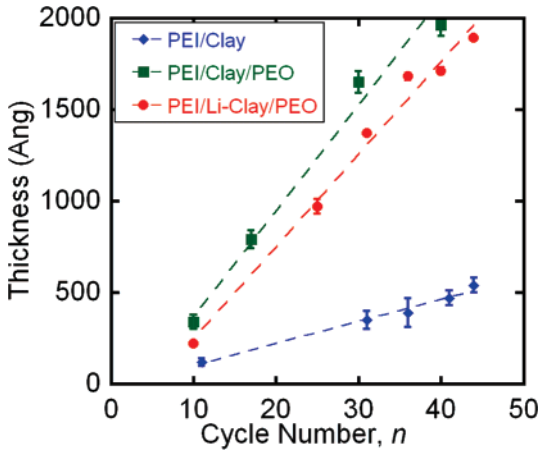

Figure 1. Growth profiles of PEI/clay, PEI/clay/PEO, and PEI/Li-clay/PEO from ellipsometry and profilometry show that films grow linearly with 11, 54, and 47 Å of material per trilayer, respectively.

Samples probed at 53% humidity were enclosed in a sealed chamber with magnesium nitrate hexahydrate salts to maintain humidity. For dry measurements, an argon-filled glovebox with ~2 ppm water was used. A home-built Faraday cage and hotplate system allowed control of cell temperature within the glovebox. In both cases, cells were allowed to equilibrate with the box environment for 24 h before electrochemical measurements.

Lithium-Exchanged Clay Preparation. Lithium-exchanged clay (Li-clay) was prepared according to Khan et al.[12] Briefly, Laponite RD clay was dissolved in Milli-Q water. Excess lithium chloride was added to the dispersion to facilitate ion exchange. The clay suspension was centrifuged, and the opaque gel was retained. The dissolution and exchange process was repeated twice more. The final gel was heated at 100 °C and then washed with methanol until a drop of silver nitrate in the effluent remained clear to confirm the complete removal of chloride ions. The resulting white powder was dried at 80 °C to give the final product, Li-clay, with a calculated yield of 60 wt %.

Results and Discussion

Multilayer Growth Mechanism and Rate. In a desire to produce an LbL film composed of a polymer electrolyte and a single-ion conductor, negatively charged Laponite clay was selected as a well-investigated and robust single-ion conductor.[12] In this study, neutral PEO and positively charged linear PEI were both selected as candidate polymer electrolytes.[24] PEI[47] and PEO,[48] owing to their polar backbones, have demonstrated promising ionic conductivities when used as a component in electrostatic[47] and hydrogen bonding[48] LbL electrolyte films. Attempts to create LbL structures from neutral PEO and negatively charged Laponite clay were unsuccessful, owing to the formation of a thixotropic gel during deposition. Also, multilayer formation from positively charged PEI and neutral PEO was unsuccessful.

Film thickness as a function of cycle number *n* was investigated using profilometry and ellipsometry for three systems: (PEI/clay), (PEI/clay/PEO), and (PEI/Li-clay/PEO). Figure 1 demonstrates a representative growth profile for these three systems, where each film thickness was measured after drying. In each case, a linear slope was obtained, where the thickness per cycle was taken as the slope of the growth profile (Table 1).

The shape of the growth profile of each composite resembled previously reported curves for polymer−clay layer-by-layer assemblies.[33,41] At early deposition cycles, little growth was observed because initial layers of polymer and clay form nucleation islands until a uniform coating covers the substrate.[49] After 10 trilayers, the substrate no longer affects polymer and clay adsorption, and film growth proceeds uniformly. The observed linear growth profile suggests that each cycle results in the deposition of the same amount of material on the substrate.

Table 1. Thickness per LbL Cycle

LbL system	Å per cycle
PEI/clay/PEO	54 ± 4
PEI/Li-clay/PEO	47 ± 3
PEI/clay	11 ± 2
PEO/clay	–
PEI/PEO	–

The cycle thickness for each of the three systems implies that the clay platelets adsorb in flat or slightly tilted layers. Given a cycle thickness of 54, 47, or 11 Å (Table 1) and a manufacturer-reported platelet diameter of 30 nm, we calculated using Pythagorean theorem that a single clay platelet may tilt as much as 10, 9, or 2°, respectively, relative to the substrate (Supporting Information and Figure 1). This behavior can be explained by the negative charge associated with the platelet face.[50] By aligning face-down, platelets can maximize interaction with the positively charged PEI layer. In contrast, the platelet edge has a positive polarity[50] that discourages edge-up adsorption.

Both neat and lithium-exchanged clay composites produced smooth films, as measured by profilometry. A film of $(PEI/clay/PEO)_{40}$ exhibited a root-mean-square (rms) roughness of 2.4 nm, and a film of $(PEI/Li\text{-}clay/PEO)_{40}$ exhibited an rms roughness of 3.0 nm by profilometry.

Because films of only PEO and clay were gel-like and unprocessable, we sought to include a third component that would stabilize film formation via mutual interactions between PEO and clay. PEI, partially charged at pH 5,[47] was chosen as the stabilizing component because of its ability to interact with Laponite via electrostatic interactions and PEO via ion−dipole interactions and hydrogen bonding. For comparison, cycle thickness increases from 11 Å for (PEI/clay) to 54 Å for (PEI/clay/PEO), which is indicative of incorporation of PEO in the stabilized LbL film.

We hypothesize the following mechanism for film formation in the PEI/clay/PEO trilayer system. Positively charged PEI adsorbs from solution to a negatively charged silicon substrate to yield a positive substrate surface charge. Negatively charged Laponite then adsorbs to the PEI-coated substrate, reversing the surface charge. Third, PEO adsorbs to the Laponite-coated surface from solution. It is believed that PEO and clay associate through hydrogen bonding and the desorption of water along the platelet surface.[21,22] These three steps comprise a single deposition cycle, resulting in a single trilayer of PEI/clay/PEO. Weak association between PEO (deposited during the *n*th deposition cycle) and PEI (deposited during the $n + 1$ cycle) through ion−dipole interactions and hydrogen bonding ensures adhesion between successive trilayers. Thus, positively charged PEI is used to associate with both negatively charged Laponite and hydrogen-bonding PEO to create stable and cohesive thin films.

Film Characterization. X-ray photon spectroscopy (XPS) of $(PEI/Li\text{-}clay/PEO)_{60}$ was used to quantify the composition of the LbL assembly. On the basis of the relative XPS signals of magnesium from the clay and carbon and nitrogen from the polymers, the LbL assembly contained 66, 30, and 4 wt % Li-

(48) DeLongchamp, D. M.; Hammond, P. T. *Langmuir* **2004**, *20* (13), 5403−5411.

(49) Jeon, J.; Panchagnula, V.; Pan, J.; Dobrynin, A. V. *Langmuir* **2006**, *22* (10), 4629−4637.

(50) Baghdadi, H. A.; Sardinha, H.; Bhatia, S. R. *J. Polym. Sci., Part B: Polym. Phys.* **2005**, *43* (2), 233−240.

clay, PEO, and PEI, respectively, when clay was the topmost layer as well as when PEO was the topmost layer. Lithium atoms could not be detected owing to their low concentration and the weak XPS signal of the Li 1s orbital. Of note, sodium was present in low concentrations, 0.04 wt %, and chlorine was undetectable.

Tapping mode AFM characterized the surface features of an LbL film of $(PEI/clay/PEO)_{60}$ in which clay was the topmost layer. Circular and oblong features were observed in both the height and phase images (Figure 2a,b, respectively). The diameters of these features (40 to 60 nm) are slightly larger than the manufacturer's reported diameter of the clay platelet (30 nm), though this difference may be attributed to artifacts from the cantilever tip. Rms roughness from an 800-nm square height image was 3.5 nm, whereas profilometry gave a roughness of 2.4 nm.

Cross-sectional SEM (Figure 2c) of a $(PEI/Li\text{-}clay/PEO)_{200}$ assembly further suggests our proposed layered structure. Bright regions are associated with clay platelets, while dark regions are likely polymer. In the micrograph, the edges of individual clay platelets appear to lay parallel to the silicon substrate, while the top of the multilayer film appeared edge-on as a smooth surface. This micrograph is similar to images reported for layered montmorillonite/PDAC LbL structures.[40]

Structural Analysis Using WAXD and GI-SAXS. WAXD was performed on neat Laponite powder, an LbL film of $(PEI/Clay/PEO)_{60}$, and an LbL film of $(PEI/Li\text{-}clay/PEO)_{60}$ in which clay was the topmost layer for both films. Figure 3a shows the $\theta-2\theta$ plot obtained from WAXD. Neat Laponite powder exhibited one shoulder and three distinct peaks in the scan range shown, consistent with previous reports of Laponite.[51] The low-angle shoulder at 6.8° corresponds to a basal (001) spacing of 13.0 Å, which is considered the periodic distance from platelet to platelet. For example, if the platelets are 1-nm thick, as reported by the manufacturer, the gallery spacing (or the distance between stacked platelets) is 3 Å. The Scherrer equation,[52] which estimates crystallite size or range of order, could not be used here because the shape of the basal reflections was not well-defined.

In the $(PEI/clay/PEO)_{60}$ film, the low-angle peak shifted to 6.3° with a basal spacing of 14.0 Å, where the distance between platelets increased slightly to 4 Å. Two low-intensity higher-angle peaks (19.3 and 26.2°) appear at angles similar to those observed in neat Laponite (20.0 and 28.0°). Multilayers containing lithium-exchanged Laponite, (PEI/Li-clay/PEO), exhibited peaks identical to multilayers containing unlithiated clay, (PEI/clay/PEO).

Further evidence of the (PEI/Li-clay/PEO) structure was obtained using GI-SAXS (Figure 3b), which measures the orientation of periodic structure within a thin film. The off-specular scattering can be analyzed for incidence angles close to the critical angle of total external reflection of the composite, revealing both lateral structure within the film and structure normal to the substrate.[53] The peak scattering intensity was observed at $q = 4.48\ nm^{-1}$, corresponding to a basal spacing of 14 Å, which is similar to our WAXD observation. Because the observed scattering was preferentially along the film normal, the results suggest that Laponite platelets are oriented parallel to the substrate. The Hermans orientation parameter (f)[46,54] was used to quantify the degree of orientation within the LbL assembly. This parameter ranges from 1 to −1/2, in which a value of zero indicates a completely random distribution of orientations. When f is 1 or −1/2, the system is completely aligned parallel or perpendicular, respectively, to the chosen reference direction (in this case, normal to the substrate). The intensity of the scattering at the scattering vector **q** in question was analyzed, and the Hermans orientation parameter was found to be 0.7, indicating that the platelets within the LbL assembly have significant, but imperfect, orientation parallel to the silicon substrate.

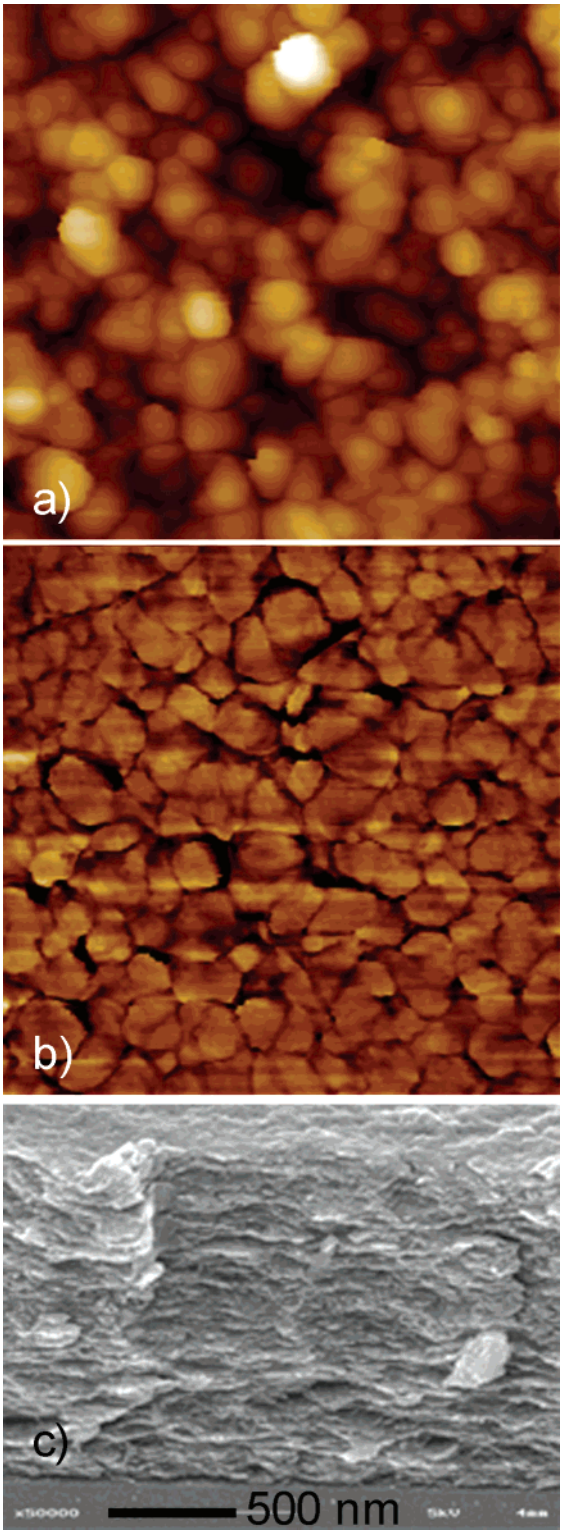

Figure 2. AFM height (a) and phase (b) images of a $(PEI/clay/PEO)_{60}$ film where clay is the top most layer, 800 nm square with 30 nm and 30° scale. (c) Cross-sectional SEM of $(PEI/Li\text{-}clay/PEO)_{200}$.

(51) Le Luyer, C.; Lou, L.; Bovier, C.; Plenet, J. C.; Dumas, J. G.; Mugnier, J. *Opt. Mater.* **2001**, *18* (2), 211−217.
(52) Warren, B. E. *X-Ray Diffraction;* Addison-Wesley: Reading, MA, 1969.
(53) Busch, P.; Rauscher, M.; Smilgies, D.-M.; Posselt, D.; Papadakis, C. M. *J. Appl. Crystallogr.* **2006**, *39* (3), 433−442.
(54) Finnigan, B.; Jack, K.; Campbell, K.; Halley, P.; Truss, R.; Casey, P.; Cookson, D.; King, S.; Martin, D. *Macromolecules* **2005**, *38* (17), 7386−7396.

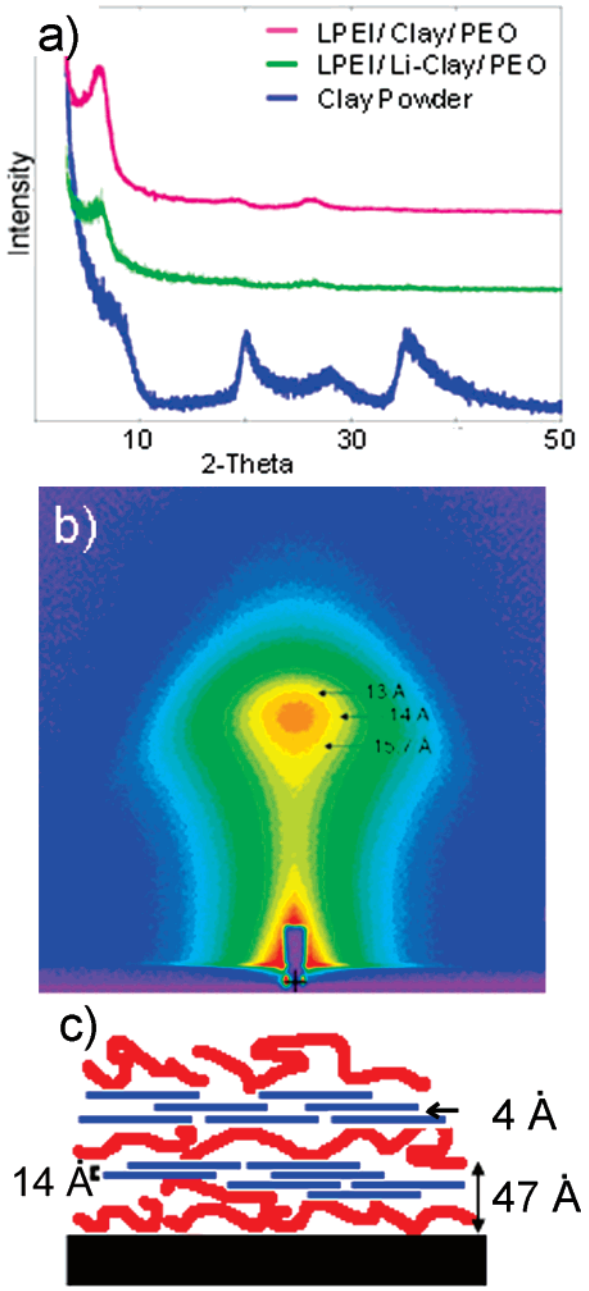

Figure 3. (a) WAXD of Laponite clay powder in blue (bottom), PEI/Li-clay/PEO in green (middle), and PEI/clay/PEO in pink (top). (b) The shape of the GI-SAXS pattern of PEI/Li-clay/PEO indicates orientation parallel to the substrate surface. (c) Proposed structure of PEI/Li-clay/PEO LbL assembly. The trilayer thickness is 47 Å (from growth profile), the basal spacing is 14 Å (from GI-SAXS and WAXD), and the gallery spacing is 4 Å (basal spacing minus clay platelet thickness, 14 Å − 10 Å = 4 Å).

The peaks from the LbL assemblies observed in WAXD and GI-SAXS suggest periodic structure within the film (i.e., the clay is not exfoliated). The small increase in gallery spacing from 3 to 4 Å (neat Laponite and PEI/Li-clay/PEO, respectively) does not indicate complete intercalation of polymer between individual platelets; however, the presence of the low-angle peaks indicates that, for each clay-deposition step, clay platelets are adsorbed in multiple layers, not a monolayer. Given an LbL assembly growth rate of 47 Å per trilayer (from ellipsometry and profilometry), a periodic length scale of 14 Å from clay platelet-to-platelet (from WAXD and GI-SAXS), lateral orientation (from GI-SAXS), and at least two layers of clay adsorbed per trilayer

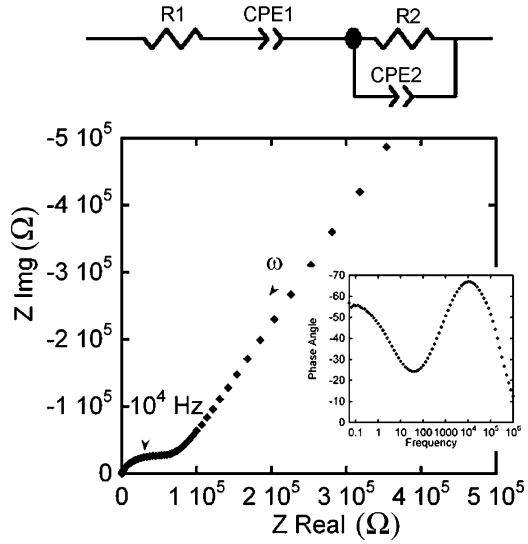

Figure 4. Representative Nyquist and Bode (inset) plot of (PEI/Li-clay/PEO)$_{60}$ at 170 °C. Data fit to above model give an electrolyte resistance (R2) of 62 000 Ω. With a cell constant of (L/A) = 0.0045 cm^{-1}, the resulting conductivity is 7.3 × 10^{-9} S cm^{-1}.

cycle (from WAXD and GI-SAXS), we propose that the multilayer structure of PEI/Li-clay/PEO consists of alternate, stratified layers of polymer and clay. From XPS, it is believed that the majority of the polymer content to be PEO (as stated earlier, multilayers contained 66, 30, and 4 wt % Li-clay, PEO, and PEI, respectively). We hypothesize that anisotropic structure of the LbL film, as confirmed by AFM, SEM, WAXD, GI-SASXS, and growth profiles, influences ionic conductivity with respect to orientation. This was investigated using EIS, detailed below.

Ionic Conductivity and Electrochemical Impedance Spectroscopy. EIS is a useful tool for investigating the movement and transport of ions (e.g., conductivity) within an electrolyte. Multilayered composites of (PEI/Li-clay/PEO)$_{60}$ were probed using EIS to measure ionic conductivity as a function of temperature, humidity, and orientation. Both cross-plane and in-plane conductivities were investigated at 53% and 0% relative humidity (RH).

The impedance response of (PEI/Li-clay/PEO)$_{60}$ was measured in two different cells to isolate the cross- and in-plane directions. Cross-plane (z direction) ion transport was measured in a cell consisting of multilayers deposited on patterned ITO glass and gold electrodes evaporated atop the multilayer film; in-plane ($x-y$ direction) ion transport was measured using independently addressable ITO microband electrodes (IAMEs). A typical Nyquist plot for a cross-plane cell (Figure 4) gave a depressed semicircle at high frequency and a near-vertical line at lower frequency, which is similar to previous reports of PEO−clay composites;[7] in-plane measurements gave a similar response. This high frequency behavior, previously described,[4,12] is best modeled using a resistor and constant-phase element (CPE) in parallel, preceded by a resistor and CPE in series to capture low frequency domains (equivalent circuit in Figure 4). R1 and R2 represent the electrode resistance and multilayer assembly resistance, respectively. CPE1 describes the nonideal capacitive double layer, most likely caused by a rough electrode−electrolyte interface, and CPE2 corresponds to bulk polarization of the LbL film. To check cell design and self-consistency, samples of varying thickness (200−300 nm) were constructed; electrolyte resistance, R2, scaled linearly with thickness, as expected.

Given the equivalent circuit, described above, and the impedance response of our multilayers at 53% and 0% RH and

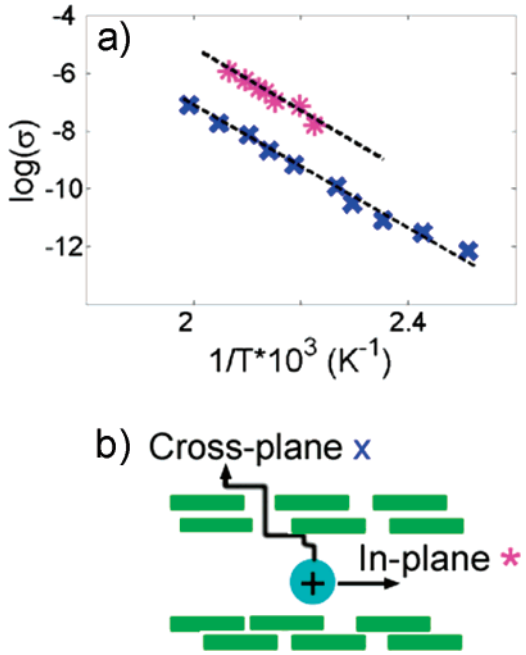

Figure 5. (a) Arrhenius plot of the variation of conductivity with temperature from 30 to 200 °C of (PEI/Li-clay/PEO) assemblies in a dry argon glovebox. In-plane conductivity (pink *) is consistently 100 times higher than cross-plane conductivity (blue x). The similar slopes (dashed lines) indicate comparable activation energies of 0.35 and 0.37 eV for cross- and in-plane conductivities, respectively. (b) Cross-plane ion conduction is hindered by the presence of ordered clay nanoplatelets, while in-plane ion conduction is unhindered.

Table 2. In-Plane and Cross-Plane Conductivity at 0% and 53% RH and 25 °C

orientation	σ (S cm^{-1}) at 53% RH	σ (S cm^{-1}) at 0% RH
in-plane (z)	$2.6 \pm 0.2 \times 10^{-7}$	*a*
cross-plane ($x-y$)	$4 \pm 1 \times 10^{-8}$	$7 \pm 1 \times 10^{-13}$

[a] Exceeded limits of impedance analyzer.

25 °C, we calculated in- and cross-plane conductivity (Table 2) using $\sigma = L/(R2 \cdot A)$, where L is the distance between electrodes and A is the area between electrodes. The ratio of the in- and cross-plane measurements gives the anisotropy factor; films at 53% RH exhibited an anisotropy factor of 7 (from Table 2). The anisotropy factor for films at 0% RH and 25 °C could not be calculated because in-plane measurements at these conditions exhibited impedance that exceeded the limits of the analyzer. Of note, while electrode resistance (R1) remained constant with increasing humidity, the multilayer resistance (R2) dramatically decreased (i.e., LbL conductivity increased). This behavior can be explained by the presence of water within the LbL assembly: at 53% RH, the ionic conductivity is expected to be primarily protonic because water adsorbed along the platelet faces is predominately acidic;[55] however, in dry conditions, the solvated cation, Li^+, is considered the mobile species.[6,7]

To further understand ion transport in $(PEI/Li\text{-}clay/PEO)_{60}$ in the dry state (0% RH), in- and cross-plane conductivities were measured as a function of temperature (30−200 °C). The temperature response of both cross- and in- plane conductivities (Figure 5a) exhibited Arrhenius behavior. Results were reproducible from sample to sample with no hysteresis from thermal cycling. Below 115 °C, the impedance of the IAMEs for in-plane measurements exceeded the limits of the analyzer. The activation energies, which are related to the slope of $\log(\sigma)$ vs $1/T$, for in- and cross- plane conductivities were 0.37 and 0.35 eV (36 and 33 kJ/mol), respectively; these numbers compare well with the activation energy of Li^+ in PEO, which ranges from 0.2 to 0.3 eV.[56,57] Alternatively, the activation energy for ion transport in Li^+−montmorillonite is ∼1 eV.[7] Given an observed activation energy of 0.35−0.37 eV and assuming Laponite behaves similarly to montmorillonite, we propose that ion transport in (PEI/Li-clay/PEO) mirrors that of Li^+ transport in PEO. Because both in- and cross-plane activation energies are similar to that of Li^+−PEO, we propose that chain segments of PEO may participate in the cross-plane ion transport process as PEO serves to bridge between clay platelets.

Despite the similar in- and cross-plane conduction activation energies, cross-plane conductivity was 100 times less than in-plane conductivity (Figure 5a). This is explained by the tortuous path the small lithium ion ($r = 0.68$ Å) must travel to migrate in the z-direction (Figure 5b), weaving around oriented clay platelets ($r = 15$ nm). Further evidence of a tortuous path is present in differences observed in α of the CPE2, $Z_{CPE} = 1/[Q \cdot (j\omega)^{\alpha}]$. The CPE represents a distribution of time constants for ion transport, and the resistive or capacitive character of the response is described by α, which ranges between 0 and 1.[58] In-plane measurements were nearly capacitive with $\alpha = 0.97$, meaning there is one mode of ion transport. Cross-plane measurements, $\alpha = 0.7$ to 0.8, were less capacitive in character and pointed to mixed time constants of ion transport. Indeed, in the cross-plane, multiple time constants are possible because an ion has many tortuous paths to choose from, whereas with in-plane conduction, ion transport occurs relatively uninterrupted in one direction.

As suggested by Ruiz-Hitsky and Aranda and others,[6,13−15] polymer−clay composites are single-ion conductors. The relatively large anionic clay nanoplatelets are virtually immobile compared to the facile lithium ion, yielding an ideal lithium transference number of unity. The LbL films discussed here are potential single-ion conductors, where the lithium cation is solvated by PEI and PEO[24] and charge balanced by negatively charged Laponite clay. However, we were unable to measure the transference number of the LbL system because a cell of Li|LbL-film|Li, necessary for this measurement, could not be constructed owing to difficulties in isolating the LbL film. Future efforts aim at resolving the challenge of lifting-off or isolating the film to allow the measurement of the transference number as well the mechanical and transport properties.

Conclusion

In summary, polymer−clay nanocomposites of PEI, Laponite clay, and PEO were constructed using LbL assembly technique; each trilayer was ∼5 nm in thickness, and clay platelets appeared to lay face-down relative to the substrate. Anisotropic structure of the films was confirmed using multiple techniques (GI-SAXS, WAXD, AFM, SEM). This system is thought to be built upon hydrogen bonding and electrostatic interactions among the three components. Anisotropic ion transport, resulting from anisotropic structure, was investigated using EIS, which demonstrated in-plane ionic conductivities 100 times faster than cross-plane conductivities (at 0% RH). The activation energy associated with

(55) Slade, R. C. T.; Barker, J.; Hirst, P. R.; Halstead, T. K. *Solid State Ionics* **1987**, *24* (4), 289−295.

(56) Robitaille, C. D.; Fauteux, D. *J. Electrochem. Soc.* **1986**, *133* (2), 315−325.

(57) Chung, S. H.; Jeffrey, K. R.; Stevens, J. R. *J. Chem. Phys.* **1991**, *94* (3), 1803−1811.

(58) Orazem, M. E. *Impedance Spectroscopy Short Course*, 209th Meeting of the Electrochemical Society, Denver, CO, May 7, 2006; The Electrochemical Society: Denver, CO, 2006; pp 3−9.

ion transport in (PEI/Li-clay/PEO) (0.35−0.37 eV) at 0% RH was similar to that of lithium cations in PEO. When humidity was increased from 0% RH to 53% RH, observed cross-plane conductivity increased (from 7×10^{-13} to 4×10^{-8} S cm^{-1}, respectively) and the degree of anisotropic transport decreased (from 100 to 7, respectively) at 25 °C. With regard to LbL assemblies, this study represents a first correlation of structural anisotropy to transport anisotropy using EIS.

Recommendations for refining the PEI/clay/PEO system for practical use as an electrolyte include (1) adding a plasticizer such as ethylene carbonate (increasing charge mobility), (2) adding a Li^+ salt to increase Li^+ concentration, and (3) creating exfoliated or disorganized LbL films containing polymer electrolyte and Laponite clay (thus removing the anisotropy). In light of the demonstrated influence on ionic conductivity, the anisotropic structure of this LbL film system may allow introduction of anisotropy in gas permeability or mechanical properties for additional applications.

Acknowledgment. We thank the Dupont-MIT Alliance for funding. We thank the Institute of Soldier Nanotechnology, Center for Materials Science and Engineering, and Prof. Yang Shao-Horn for facilities. We thank Dr. Piljin Yoo and Kathleen McEnnis for their assistance. Dr. Lutkenhaus thanks the National Science Foundation Graduate Fellowship for support. This work is based upon research conducted at the Cornell High Energy Synchrotron Source, which is supported by the National Science Foundation and the National Institutes of Health/National Institute of General Medical Sciences under Award DMR-0225180.

Supporting Information Available: Tilted platelet graphic. This material is available free of charge via the Internet at http://pubs.acs.org.

LA700432P